Experiments on the hypersonic turbulent shock-wave/boundary-layer interaction and the effects of surface roughness

S. A. Prince,
Centre for Aeronautics
City University
London

M. Vannahme and J. L. Stollery
College of Aeronautics, Cranfield University
Cranfield, UK

ABSTRACT

An experimental investigation was performed to study the effects of surface roughness on the Mach 8·2 hypersonic turbulent shock-wave–boundary-layer interaction characteristics of a deflected control flap configuration. In particular, the surface pressure and heat transfer distribution along a quasi-2D ramp compression corner model was measured for flap angles between 0° and 38°, along with a Schlieren flow visualisation study. It was found that surface roughness, of scale 10% of the hinge-line boundary layer thickness, significantly increased the extent of the interaction, while increasing the magnitude of the peak pressure and heat flux just aft of reattachment. The incipient separation angle for a fully turbulent, Mach 8·2 boundary layer with a hinge line Reynolds number of $1{\cdot}44 \times 10^6$, was estimated at 28-29°, reducing to between 19-22° with the introduction of laminar sub-layer scale surface roughness.

NOMENCLATURE

C_H	heat transfer coefficient, $q/\rho u C_P(T_r - T_w)$
C_P	specific heat at constant pressure (J/kgK)
L	plate length (m)
M	Mach number
p	static pressure (N/m²)
q	surface heat transfer rate (W/m²)
T	temperature (K)
u	local velocity (ms⁻¹)
x	axial distance from plate leading edge (m)
y	normal distance from model surface (m)
ξ	non dimensional distance $(x\text{-}L)/\delta$
β	flap deflection angle (deg)
δ	boundary layer thickness (m)
ρ	density (kg/m³)

Subscripts

r	adaibatic wall conditions
R	location of boundary-layer reattachment
S	location of boundary-layer separation
w	conditions at the model surface
∞	conditions at free stream

1.0 INTRODUCTION

Recent developments in re-entry space plane and guided missile and projectile technologies, have focused interest on the flow phenomena specific to the hypersonic flight regime. During the re-entry of a reusable space plane, and the manoeuvre of a hypersonic guided weapon, the vehicle is subjected to very high heat transfer rates not only in the nose region but also in the regions of the interaction between shock waves and boundary layers.

Paper No. 2913. Manuscript received 7 September 2004, accepted 26 January 2005.

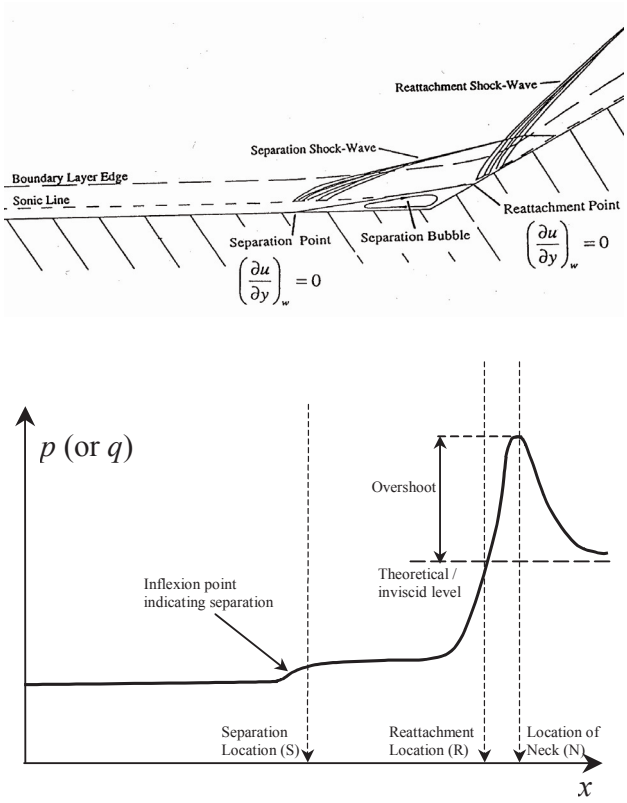

Figure 1. Schematic of the shock-wave—boundary-layer interaction at a hypersonic compression corner and associated pressure/heat transfer distribution.

One of the main regions where such interactions take place is in the vicinity of deflected control surfaces, which are required for the control and manoeuvring capability of the vehicle. During re-entry, in particular, the vehicle will experience very low density flow, and so very high flap angles are necessary to generate the required control forces. This results in very high adverse pressure gradients, and may cause flow separation upstream of the control surface, and the generation of a multiple shock-wave pattern. The resulting recirculation zone of slow moving air reduces the effective area of the control flap, and significantly increases the local heating rates.

In order to size the thermal protection systems in such regions, it is necessary to predict the peak heating induced by the interactions. Much work has been performed, both experimentally and computationally, toward the goal of an accurate capability to describe the physics of such flows[1-13]. Solutions of the full Navier-Stokes equations have proven successful in the accurate prediction of steady laminar shock wave/boundary layer interaction physics. The understanding and accurate simulation of turbulence and its unsteady effects, however, still eludes the scientific community.

The effect of surface roughness, which can develop during hypersonic flight due to the mechanism of ablation, poses a particular problem. Several investigators have studied these effects experimentally using various models for roughness, from small hemispherical bumps to sand paper distributed evenly over the model surface[15-20].

This investigation addresses the effects of roughness on control effectiveness at hypersonic speeds by focussing on the simplified model represented by the two-dimensional ramp compression corner with smooth and roughened surfaces.

2.0 HISTORICAL REVIEW

2.1 Shock wave/boundary-layer interactions

In cases of a shock/boundary-layer interaction, the deflected ramp generates an adverse pressure gradient. In the inviscid case, this would take the form of a single shock discontinuity originating at the corner of the ramp. For viscous flow, however, the boundary layer growing along the flat plate upstream of the corner will be 'aware' of the ramp deflection by pressure waves fed upstream through the subsonic portion, close to the surface of the plate. This leads to an associated pressure rise in this layer upstream of the compression corner.

For small ramp deflections, a weak shock-wave extends into the supersonic portion of the boundary layer, curving down towards the surface due to the Mach number gradient. The subsonic layer will then face a continuous pressure rise, causing the streamlines to diverge, increasing its thickness. This results in a deflection of the external supersonic/hypersonic stream, which in turn causes the development of a system of compression waves which eventually coalesce to join with the outer 'inviscid' shock-wave.

As the ramp deflection is progressively increased, the oncoming boundary layer encounters an increasingly adverse pressure gradient. When the boundary layer can no longer overcome this adverse pressure gradient, incipient flow separation occurs, and the structure of the flow is changed significantly, as illustrated in Fig. 1.

As the ramp deflection increases further, the flow will become increasingly more separated and a recirculation bubble develops. A separation compression fan develops well upstream of the hinge line, and a reattachment compression fan is generated as the free shear layer approaches the reattachment point and begins to turn parallel to the ramp surface. This compression fan eventually coalesces and interacts with the separation shock wave to form the equivalent 'inviscid' oblique shock wave.

At hypersonic speeds, the interaction of the two shocks generates an expansion fan back towards the ramp and a slip line, across which an entropy jump occurs. Downstream of the reattachment, the boundary layer reduces to a minimum thickness known as the 'neck' region, beyond which it grows back towards a self-similar form.

The state of the oncoming boundary layer for a given ramp deflection defines the extent of the interaction region. A laminar boundary layer is less energetic than its equivalent turbulent boundary layer, and so will be less capable of withstanding the adverse pressure gradient. Incipient separation angles for a laminar boundary layer are therefore much smaller than for a turbulent one.

In well separated cases the maximum pressure gradients (inflexion points in the surface pressure distribution) occur at the separation and reattachment points. A pressure overshoot aft of reattachment occurs in the vicinity of the neck region of the boundary layer, followed by a relaxation to the inviscid pressure level. Between separation and reattachment there can be either a kink in the pressure profile when the interaction region is small, or a pressure plateau for larger extents of separated flow.

The skin friction distribution exhibits negative values over the interaction region, associated with the reversed flow in the separation bubble. For the turbulent cases of interest to this investigation, the heat transfer distribution follows the same trend as the pressure distribution.

Much work has previously been done on hypersonic 2D compression corner interactions[3-12]. Elfstrom[3,4] measured the smooth surface pressure distribution beneath a turbulent boundary layer flowing over a ramp compression corner. Elfstrom found that, for attached flow cases, the pressure rise upstream of the hinge line indicated an upstream influence of less than one boundary layer thickness, associated with a thin subsonic region in the approaching boundary layer.

For separated cases with large separation bubbles there was found to be a pressure overshoot of increasing magnitude with ramp angle, which occurred just downstream of reattachment. Elfstrom attributed this phenomenon to the intersection of the separation and reattachment

https://doi.org/10.1017/S0001924000000683 Published online by Cambridge University Press

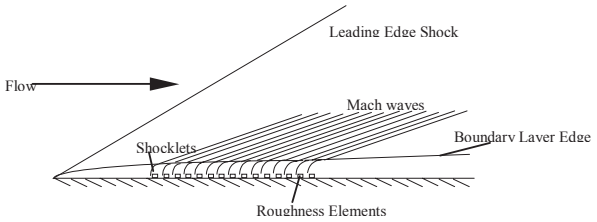

Figure 2. Shocklet formation off roughness elements.

shocks close to the surface, and suggested that its appearance could serve as an indicator for the existence of separated flow at the corner. These pressure overshoots have not, in general, been observed in supersonic ($M < 5$) flows of this type, probably because the separation and reattachment shocks do not intersect close to the surface.

Direct determination of the separation position is not an easy matter. The separation point is defined as the position where the local skin friction is zero. The angle of incipient separation is when the skin friction first drops to zero close to the hinge line. Direct determination, therefore requires the accurate measurement of the local skin friction along the surface. An alternative method is the measurement of surface heat transfer, which for turbulent flow increases in separated regions, thus effectively indicating boundary layer separation[5-7].

Coleman[5] performed an experimental investigation similar to that of Elfstrom. For the same test conditions, and using similar model configuration, he measured surface heat transfer distributions. The comparison between the pressure and heat transfer distributions was addressed by Coleman and Stollery[6,7] who concluded that the form of the two profiles are strikingly similar. The heat transfer distributions were also found to exhibit an overshoot associated with boundary layer separation at the corner, which could also be used for the determination of incipient separation.

2.2 Roughness effects

The effect of distributed surface roughness of approximately 10% of local boundary layer thickness is of primary concern in the present investigation. Much work has been done on the effect of roughness on incompressible flows in pipes and on flat plates[14], but only a limited number of studies have been performed on the effect of roughness on fully turbulent boundary layers in supersonic and hypersonic flow[15-20].

Bertin, Hayden and Goodrich[15] investigated the effect of distributed roughness on boundary-layer transition on the Space Shuttle orbiter configuration. They found that for a given size of roughness element, with grit simulating the tile misalignment, the roughness did not significantly affect the heat transfer in regions of fully laminar or fully turbulent flow on the flat plate type configuration of the windward surface of their model.

Disimile and Scaggs[16] studied the effects of roughness on the Mach 6 compressible turbulent boundary layer characteristics in the presence of a 22° ramp deflection, at three unit Reynolds numbers. The roughness consisted of machined hemispherical protuberances 0·508mm in radius. It was found that the extent of the separated region for the roughened surface was ten times that for the smooth. The smooth surface test indicated no change in the location of the separation point for the three Reynolds numbers. Additionally they found that the effect of roughness was to reduce the fullness of the boundary layer, caused by the loss of momentum in the layers closest to the wall resulting from shocklets and wakes generated by individual roughness elements.

Christoph and Fiore[17] stated that in a hypersonic boundary layer it is possible to generate shocklets – small weak shock waves associated with individual roughness elements, even for small roughness heights. The shocklets start at the sonic line, are detached and approach the flow Mach angle at the boundary layer edge, as illustrated in Fig. 2. Christoph and Fiore argued that such shocklets are very weak and suggested that they have a minor effect in reducing the strength of shock waves which may be generated downstream.

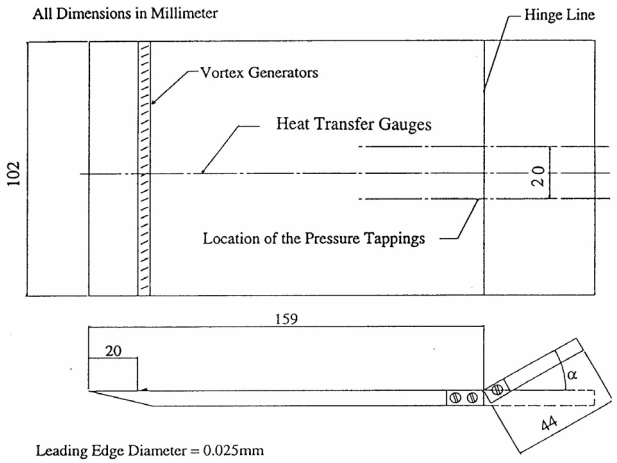

Figure 3. The experimental model configuration.

3.0 THE EXPERIMENTAL PROGRAMME

The experimental studies were conducted in the Cranfield College of Aeronautics Gun Tunnel facility[2]. This consists of an intermittent, free piston compressor feeding a blowdown hypersonic nozzle. The present experiments were performed using the Mach 8·2 convergent-divergent nozzle which produces a uniform flow in the working section. The Reynolds number can be varied in the range $4{\cdot}5 \times 10^6$/m to $9{\cdot}05 \times 10^6$/m, putting most experiments in the regime where transition to turbulence occurs. In the present investigation the Reynolds number, based on the plate length (L), was $1{\cdot}44 \times 10^6$.

A calibration exercise in the working section revealed that the tunnel provided a useful run time of 25ms, and a fully developed flow after approximately 3-4ms.

The experimental models, illustrated in Fig. 3, consisted of a steel flat plate with sharp leading edge and a hinged moveable flap. One model incorporated surface pressure tappings of 1mm diameter, 10mm either side of the centreline, while the other model incorporated thin film heat transfer gauges along the model centreline. The flap could be continuously adjusted up to a flap angle of 40°. Vortex generators were utilised 20mm from the leading edge to trip the boundary layer to a fully turbulent state. These were based on the design successfully developed by Coleman[5] and consisted of a single row of delta shaped protuberances, 1mm high and 3·5mm apart, inclined at about 30° to the flow direction. The model mounting fixed the flat plate at a position exactly in the centre of the oncoming uniform core flow from the nozzle.

The roughness under study was chosen to simulate that experienced on missiles and re-entry vehicles due to ablative effects at hypersonic speeds, and thus had to be uniformly distributed with individual elements that protrude above the corresponding smooth surface laminar sublayer. An additional criterion was that the roughness be resistant to the working section operating conditions. It was decided, after tests on a smooth surface model, that fine sand grains with an effective average roughness height of 0·3mm would fulfil these requirements. In order to avoid any interference effects or damage to the instrumentation, the surface was kept free of the 'sand grain' roughness within a 2mm distance of each pressure tapping or thin film gauge.

To test the effectiveness of the vortex generator strip in producing a fully turbulent boundary layer on the model surface, the liquid crystal thermography technique, using Licritherm TCS 811 liquid crystals manufactured by Merck-BDH, together with Schlieren flow visualisation of the boundary layer, with and without the strip, was used.

https://doi.org/10.1017/S0001924000000683 Published online by Cambridge University Press

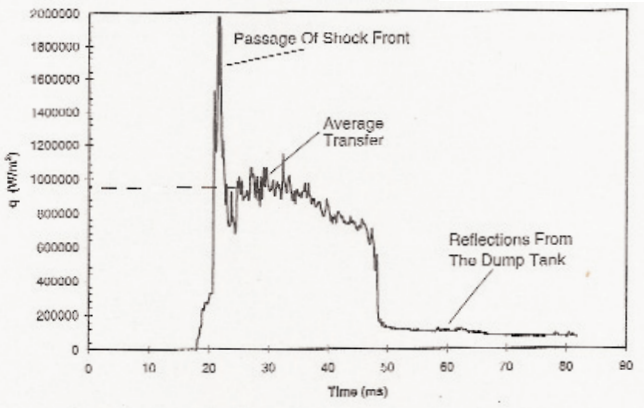

Figure 4. Typical heat transfer time response plot.

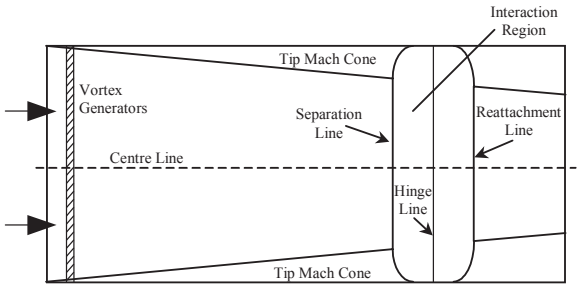

Figure 5. 3D effects due to the establishment of edge crossflow.

The effect of the roughness was investigated by three series of measurements. The surface pressure and heat transfer distributions were measured at the different flap angles for (*i*) a fully smooth surface, (*ii*) roughening only on the flat plate, and (*iii*) a roughened flat plate and flap.

3.1 Measurement instrumentation

The thin film heat transfer gauges were 1mm wide by 10mm in length and consisted of platinum strips mounted on a ceramic insert which was positioned in the model surface along its centreline. The measurement system incorporated a Thevenin circuit to provide a voltage stabilised power source and to isolate the instrumentation from the electrical noise associated with the mains system. Constant input currents of approximately 10mA were used to power the thin film gauges during the run. The voltage rise associated with the temperature rise of the gauges was integrated using a C-R analogue circuit and the output was amplified and passed through an analogue 0·02Hz-100kHz band pass filter. The heat transfer rate, which is proportional to the output voltage, was then stored on a transient recorder[2]. The gauges have been estimated to be accurate to within 5-10% between $10 < q < 500$ kW/m^2. Figure 4 presents a typical heat transfer trace during the tunnel run and shows how the average heat transfer (dashed line) was estimated, together with the electrical noise inherent in the thin film technique. The traces for the measured surface pressure were similar to those for heat transfer, but with considerably less signal noise. Both measurements presented about 10-20ms of run time during which the flow seemed to be steady.

KULITE XCS-190 series transducers of 0-15psig range were used for the pressure measurements and were connected to the tappings by PORTEX tubes. The transducers were located at the base of the model such that the tube length, and the associated response time delay, was minimal. The data recording system consisted of a low noise eight-channel amplifier coupled to a digital transient recorder. For each run the pressure-voltage calibration was performed during the evacuation phase of the tunnel. Experimental error is estimated to be less than 5%.

A single pass Schlieren flow visualisation system was used to provide an essentially two-dimensional photographic representation of the flow field. An Argon stabilised source was used to produce a high intensity beam of polarised light, together with a horizontal/vertical knife edge setup, and a Land Polaroid camera.

For each flap deflection at least two sets of pressure distribution and heat transfer distribution measurements were taken, each together with a corresponding Schlieren photograph. This was done in order to assess the repeatability of the experiments and the flow unsteadiness.

4.0 RESULTS

4.1 Flow structure

Preliminary tests on vortex generator effectiveness, using Schlieren flow visualisation and liquid crystal thermography, suggested that boundary layer transition was effectively achieved. The vortex generators were seen, in the liquid crystal surface flow visualisation study, to produce strong vortex filaments that could be traced to around 65-75% of the model length before they appeared to break-down. While photographs of the liquid crystal film response revealed distinct traces of the vortex filaments and considerable reaction to the separation shock near the hinge, the results were not deemed to be of sufficient quality to allow for direct measurement of the magnitudes of local heating rates. The performance of the liquid crystal technique for thermography is very sensitive to the quality, preparation and smooth application to the surface of interest.

The boundary layer thickness at the hinge line, seen in the Schlieren photography, was found to increase approximately threefold by the introduction of the vortex generator strip†. While further experimental studies, such as velocity measurements, could provide better evidence of the state of the boundary layer, the results of the present study, taken with those from similar studies using vortex generator strips, all point to a fully turbulent boundary layer existing on the plate surface.

Three-dimensional effects were also evident from the liquid crystal analyses. Because of the finite aspect ratio of the plates a significant portion of the hypersonic stream will be affected by the flow around the edges, causing large curvatures of the separation and reattachment lines in a manner, which reduces the interaction lengths, especially near the plate edges. An exaggerated sketch of this effect is given in Fig. 5. The curvature due to crossflow in the subsonic layer is much smaller in the region between the tip Mach cones, and the flow in this region can therefore be considered quasi-two dimensional.

The problem of three-dimensional edge effects cannot easily be remedied. The other option considered to reduce the edge effects at the centre line, where the measurements were made, was the use of edge plates. This technique would have prevented flow around the model edges, but would have introduced side-wall shock waves that would have caused flow crossflow boundary layer separation and the development of corner vortices. Given the restriction of the small working section, and the relatively small extent of the tip Mach cones seen in the liquid crystal study, it was decided not to use side walls.

The measurements of surface pressure and surface heat transfer were seen to be repeatable to within 1-5% of the maximum measured value for each pressure tapping/heat transfer gauge. In addition, the Schlieren photographs for each roughness/flap deflection case were practically identical in their definition, and location, of the major flow features.

† While boundary layers are clearly visible in Schlieren photography, the boundary layer thickness cannot be measured directly since the density gradient asymptotes to zero at the boundary layer edge. Only approximate values of δ, can be measured by means of a Schlieren system. In this study the hinge line δ was approximated, from a number of Schlieren photographs of the smooth surface flow past the model with zero flap deflection, at 4·3mm.

https://doi.org/10.1017/S0001924000000683 Published online by Cambridge University Press

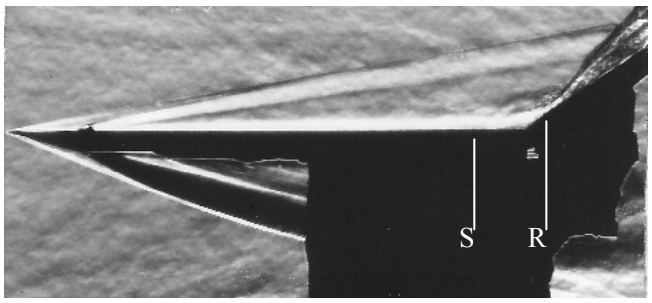

(a) Experimental Schlieren: smooth plate and flap.

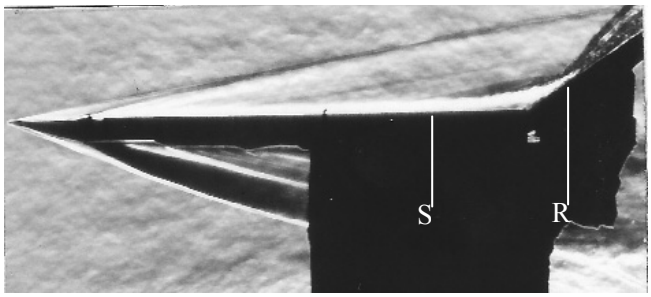

(b) Experimental Schlieren: roughened plate, smooth flap.

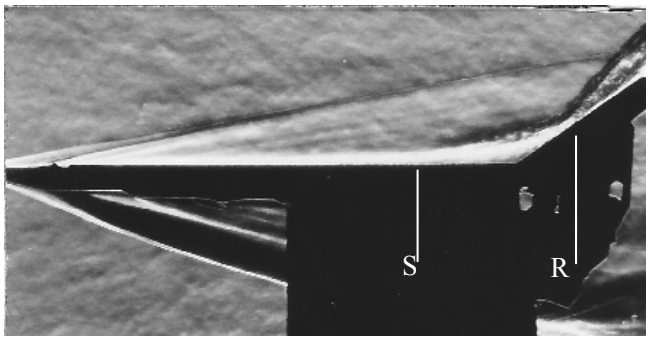

(c) Experimental Schlieren: roughened plate and flap

Figure 6. Flow structures for the three surface roughness cases at flap angle, $\beta = 35°$.

4.2 Roughness effects

Figure 6 presents a comparison of the Schlieren photographs for the 35° flap angle case, which shows the effect of the distributed surface roughness. These pictures were all taken with a horizontal knife edge, and therefore reveal vertical density gradients, highlighting shock waves and compressible boundary layers. Figure 6° displays the flow structure for the smooth surface case, which clearly shows the separation and reattachment shockwaves.

By comparison with the photographs for 30° and 25°, it was ascertained that the incipient separation flap angle was between 25° and 30° with a smooth surface. The effect of surface roughness is clearly evident in Fig. 6(b), which presents the corresponding Schlieren photograph for the case of a roughened surface on the plate alone, and shows the separation point (S) further upstream with a much more defined separation shock wave. Figure 6(c) presents the corresponding Schlieren photograph for the case with roughened flat plate and flap surfaces. Careful analysis shows that addition of roughness on the flap surface moved the position of separation further upstream and reattachment slightly (R) further downstream.

For the 25° case, a separation shock was seen to originate close to the ramp corner, approximately 15-20mm upstream. This indicates that the incipient separation flap angle for a plate roughened surface is reduced to just below 25°. For the fully roughened case, with roughness elements on both the plate and flap surfaces, a highly separated flow had already developed at 25° flap angle, showing that the incipient separation flap angle had been further reduced. The fully roughened 35° deflection flow structure exhibited a large separation bubble, with the separation location 30mm upstream of the hinge line. In addition, the reattachment position was seen to shift further downstream with the addition of roughness.

An interesting observation is the evidence, in some of the roughness cases, of lines emanating from the boundary-layer edge, which move off at approximately the Mach angle for a Mach 8·2 flow. This is consistent with the findings of Christoph and Fiore[17] and is suggested to be evidence of the shocklets formed at the sonic line.

The pressure distributions along the model surface at 25°, 30°, 35° and 38° flap angle, are presented for the three surface roughness combinations, in Fig. 7. Figure 7(a) presents the results for the smooth surface case, while the corresponding curves for the plate roughened case and the roughened plate and flap are given in Figs 7(b) and (c) respectively.

The general shapes of the profiles correspond well with the theoretical shape for a turbulent boundary layer and also with profiles obtained under different conditions by other researchers. The location of the initial surface pressure rise ahead of the corner was found to correspond well with the position of boundary-layer separation indicated by the appearance of a weak separation shock in the corresponding Schlieren photographs. As expected, the pressure rise over the deflected flap increases with deflection angle, and a pressure overshoot occurs in those cases that, from the Schlieren photographs, appear to have boundary-layer separation ahead of the corner. The location of the pressure overshoot corresponded well with the approximate location on the flap, of the neck in the boundary-layer immediately downstream of reattachment. After pressure recovery, the surface pressure was found to approach the theoretical inviscid value for the given flap deflection, to within ±6%.

The effect of surface roughness is seen to be considerable, especially for higher flap deflections. The roughness has the effect of increasing the peak pressure, associated with the 'neck' downstream of reattachment, and of shifting the position at which it occurs further downstream. This downstream movement of the neck region is approximately equivalent to the hinge line boundary-layer thickness. In addition, for the higher flap deflections, the pressure plateau, indicative of separated flow, appears very prominent in the roughened distributions for the highest flap angle.

Figure 8 presents a plot of the magnitude of the pressure overshoot downstream of reattachment, versus the flap deflection angle for the three surface roughness cases. Interestingly, the relationship between pressure overshoot and flap deflection angle, for all three roughness cases, appears to be linear, given the limited data available. The effect of roughening the flat plate was seen to be an increase in the magnitude of the pressure overshoot for a given flap deflection. Further addition of roughness to the flap surface resulted in an even greater increase in the magnitude of the pressure overshoot.

Using the pressure overshoot downstream of reattachment as a criterion to estimate the flap angle for incipient separation of the flat plate boundary layer, Fig. 8 would indicate that incipient separation for the smooth surface model occurs at about 29° flap deflection. This was found by extrapolating the linear relationship between the magnitude of pressure overshoot and flap deflection, to find the flap deflection where the pressure overshoot first becomes zero. This compares well with the results obtained by Elfstrom for a Mach 9 turbulent boundary layer, of around 30°, and with the results of Coleman who also measured the incipient separation angle for a Mach 9 turbulent boundary layer, of between 29 and 31° depending on the hinge line Reynolds number. A similar analysis of the data for the roughened plate, and the roughened plate and flap cases, reveals that the incipient separation flap angle reduces to about 27° and 22° respectively.

https://doi.org/10.1017/S0001924000000683 Published online by Cambridge University Press

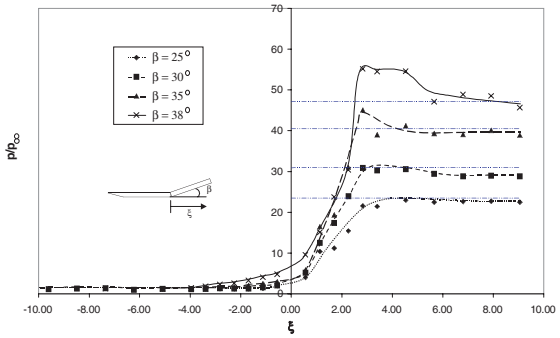

(a) Smooth plate and flap case.

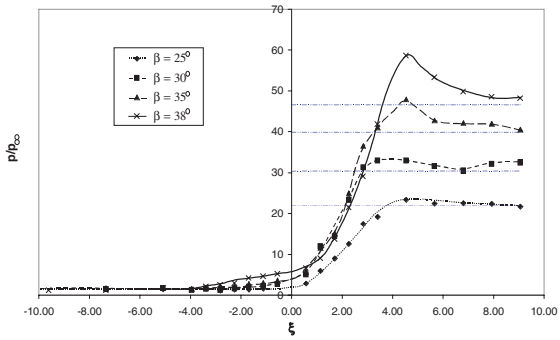

(b) Roughened plate and smooth flap case.

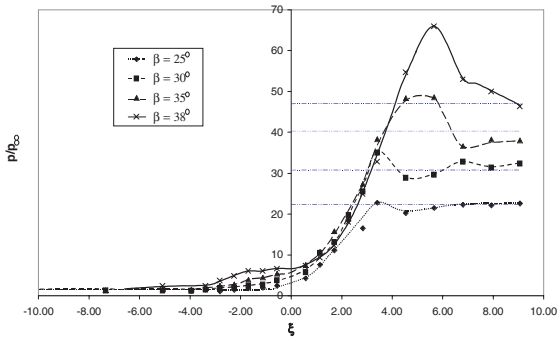

(c) Roughened plate and flap case.

Figure 7. Variation of centreline pressure distribution with flap angle for the three surface roughness conditions (inviscid levels shown by dashed lines).

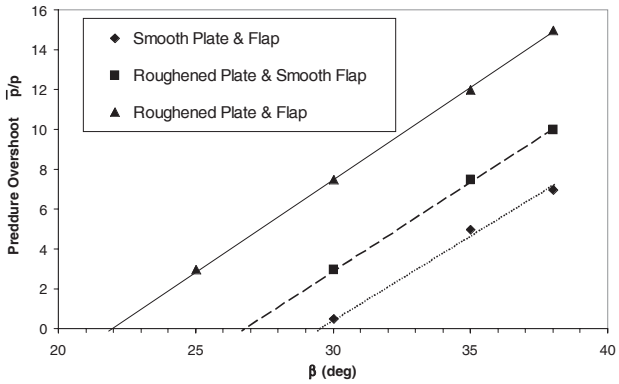

Figure 8. Variation of attachment pressure overshoot with flap angle for the three surface roughness conditions.

Similar trends were discovered in the heat transfer measurements, which are presented for the smooth, roughened plate and roughened plate and flap, cases in Figs 8(a) and 8(b) and 8(c) respectively. The peak heating rates, associated with the reattachment of the free shear layer, are significantly increased by the addition of surface roughness. The location of peak heating is also seen to move downstream by approximately one hinge line boundary-layer thickness for the roughened plate and flap case at $\beta = 35°$.

Figure 9 presents the measurements of the heat transfer rates for the three cases investigated. Despite experimental scatter attributed to electrical noise during the measurements, the heat transfer beneath the separated regions at higher flap deflections, was seen to increase in agreement with the findings of Coleman[5-7]. For the roughened cases, the heat transfer distributions in the vicinity of the separation bubble exhibited more extensive regions of higher heating rates.

One interesting observation, seen in Figs 9(b) and (c), is that the addition of roughness on the flat plate of the model appears to affect heat transfer recovery following reattachment in the case of the highest flap deflection of 35°. For these cases the heating rates downstream of reattachment failed to return to the smooth surface value seen in Fig. 9(a). Heating rates for the lower flap angles, recover to broadly the same value at $\xi = 9$, whatever the surface roughness.

Figure 10 presents the plot of the estimated location of flat plate boundary layer separation, ξ_S, and the corresponding location of shear layer reattachment on the deflected flap, ξ_R. These locations were estimated by careful examination of all of the experimental evidence. This included the surface pressure and heat transfer distributions, cross-referenced with the visual evidence provided by the Schlieren photographs. Since heat transfer is a much more sensitive indicator of boundary-layer separation and reattachment, than surface pressure, more weight was placed on the interpretation of the q measurements and the Schlieren photographs. A better analysis of the separation and reattachment locations could have been made if measurements of boundary-layer profiles or direct measurements of surface skin friction were available, but given the limited size of the facility and available instrumentation, this was impossible. However, it is suggested that the available data, with careful analysis, is sufficient to yield separation and reattachment positions to within at least $\pm 0{\cdot}5\xi$ ($\pm$2mm).

Figure 10 shows that, within the errors associated with experimental measurement and interpretation, there seems to be an almost linear relationship between the flap deflection angle and the movement of the boundary layer separation and reattachment positions. Much more data would, however, be required to confirm these findings. The available data indicates, however, that the incipient separation angle for a Mach 8·2 smooth surface turbulent boundary layer, with a hinge line Reynolds number of $1{\cdot}44 \times 10^6$, is approximately 28°. This compares with the result, obtained by analysis of the pressure overshoot, downstream of reattachment, of approximately 29°. With the addition of the surface roughness to the plate, Fig. 10 indicates the incipient separation angle is reduced to approximately 26°, compared with the figure of 27°, predicted using the pressure overshoot criterion. Further addition of roughness to the flap surface further reduced the incipient separation angle to approximately 19°, according to the results in Fig. 10, compared with a figure of about 22°, predicted from analysis of the pressure overshoot.

https://doi.org/10.1017/S0001924000000683 Published online by Cambridge University Press

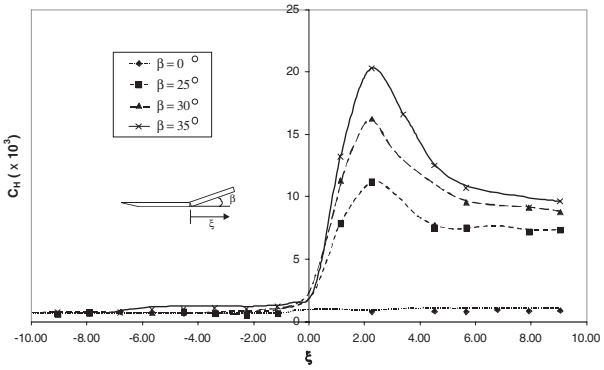

(a) Smooth plate and flap case.

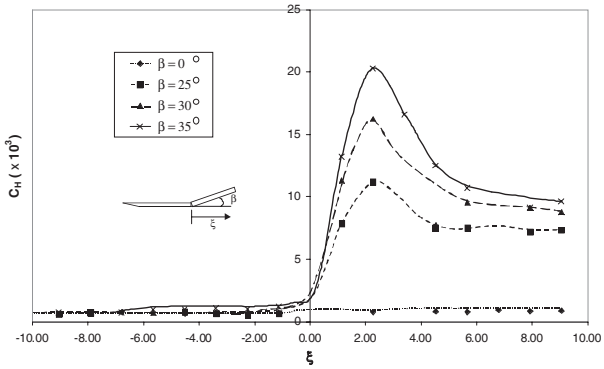

(b) Roughened plate and smooth flap case.

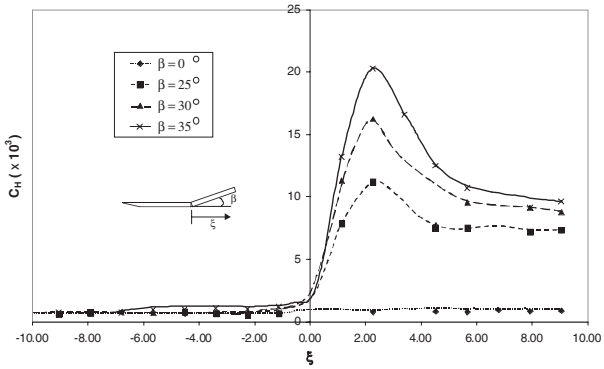

(c) Roughened plate and flap case.

Figure 9. Variation of centreline heat transfer distribution with flap angle for the three surface roughness conditions.

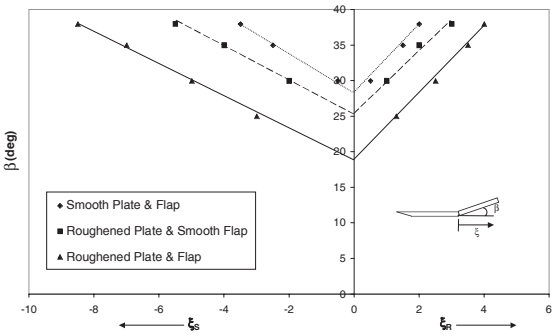

Figure 10. Variation of boundary layer separation and reattachment locations with flap deflection angle for the three surface roughness conditions.

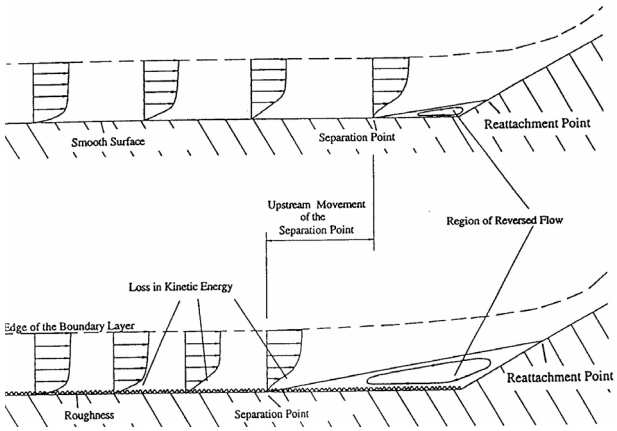

Figure 11. The effects of distributed surface roughness on the flat plate.

5.0 DISCUSSION

The results of this study, taken together, suggest that the addition of 10% hinge-line boundary-layer thickness scale roughness to the flat plate moved the turbulent boundary-layer separation point further upstream, so increasing the size of the interaction region as illustrated in Fig. 11. The angle of incipient separation was also reduced indicating that a roughened surface turbulent boundary layer is less resistant to adverse pressure gradients. This is caused by the reduction in the momentum of the inner region of the turbulent boundary layer arising from the increased shear stresses associated with the individual wakes emanating from the roughness elements.

An interesting observation is that, while the peak pressure, for roughness on the plate only, occurs about one hinge line boundary- layer thickness downstream of the smooth surface location, the corresponding movement in peak heating is only half this distance. This suggests that there is a small movement of the position of the reattachment of the separated shear layer, but a much larger movement in the location of the neck region of the attached boundary layer responsible for the pressure overshoot.

Figure 7 shows that surface roughness exerted only a minor effect on the magnitude of the peak pressure until the higher flap angles at 35° or above. The corresponding effect on the heating peak, as shown in Fig. 9, was found to be negligible with roughness on the flat plate alone, but addition of roughness to the flap as well, increased its magnitude by a maximum of 8% for a flap angle of 35°. While this 8% increase is within the accuracy of the thin film gauges (5-10%), the lack of experimental scatter at the higher heating rates, and the consistency of the results with past data suggest that the measurements are valid.

The further addition of roughness to the flap was found to move the separation point further upstream on the flat plate, thus reducing the flap deflection angle for incipient separation. The positions of both the pressure and heating peaks moved downstream by approximately the thickness of the hinge line boundary layer. This indicates a movement of the locations of both the shear layer reattachment and the neck of the subsequent boundary layer, and thus a significant increase in the size of the interaction region. These effects indicate a significant upstream effect of roughness on the flap.

It is suggested that the addition of roughness to the flap 'agitates' the reattachment process and delays the recovery of the reattached boundary layer. The effect is, initially, to move the reattachment further rearward,

https://doi.org/10.1017/S0001924000000683 Published online by Cambridge University Press

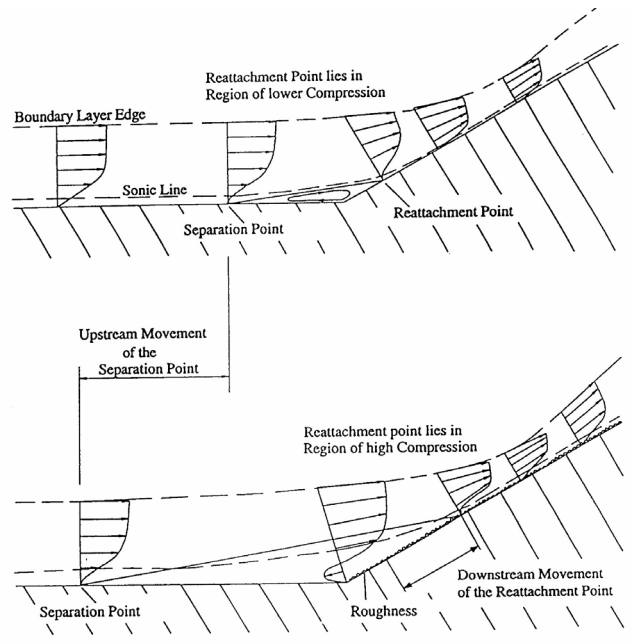

Figure 12. The effects of distributed roughness on the trailing edge flap.

extending the recirculation bubble into the region of higher pressure behind the reattachment shock and thus feeding the bubble with higher pressure disturbances. These changes in pressure are propagated through the subsonic portion far upstream on the flat plate, generating an even larger adverse pressure gradient for the approaching boundary layer to resist. The separation point will thus be moved further upstream. This mechanism is illustrated in Fig. 12.

For the case of roughness covering the entire interaction region, therefore, it is suggested that the changes in flow structure are due to a combined effect. Firstly roughness on the flat plate weakens the boundary layer upstream of the hinge line making it less resistant to the adverse pressure gradient, and secondly roughness on the flap causes a strong propagation of pressure through the separation bubble, further increasing the adverse pressure gradient on the plate.

Any upstream movement of the location of separation causes a stronger separation shock-wave and subsequent interaction resulting in a higher pressure peak close to the reattachment of the shear layer. This higher pressure is, in turn, propagated through the separation bubble causing a further upstream movement of the separation location. It is possible that this process is initially very dynamic with the separation and reattachment positions oscillating violently until a balance is reached and the flow reaches an equilibrium state.

6.0 CONCLUSIONS

The following conclusions can be derived from this study:

- The incipient separation flap angle for a Mach 8·2, fully turbulent boundary-layer flow of unit Reynolds number of $9{\cdot}06 \times 10^6$/m, was found to be approximately 28-29°. This was reduced to approximately 20° by the addition of roughness, of size equal to ~10% of the hinge line boundary-layer thickness, to the model surface.
- The addition of roughness to the flat plate was found to move the location of separation, for a given flap angle, further upstream thus extending the interaction region.
- The further addition of roughness to the trailing-edge flap moved the location of the shear layer reattachment further rearwards and the separation location further upstream.
- Surface roughness was found to have only a minor effect on the magnitude of peak pressure, resulting from the neck in the flap boundary layer, aft of reattachment, until higher flap angles above 30°.
- The effect of roughness on the peak heating rate, associated with the reattachment of the free-shear layer, was found to be small when the flat plate alone is roughened. Addition of roughness to the trailing edge flap was found to increase the peak heating rate by a maximum of 8% for a flap angle of 35°.

ACKNOWLEDGEMENTS

The authors are indebted to Prof George Inger for his advice during his visits to Cranfield, and to Wayne Osbourne for his assistance in the operation of the Gun Tunnel facility.

REFERENCES

1. PRINCE, S.A., VANNAHME M. and STOLLERY, J.L. Experiments on the hypersonic turbulent shock-wave/boundary layer interaction and the effects of surface roughness, January 1999, AIAA Paper 99-0147.
2. PRINCE, S.A. Hypersonic Turbulent Interaction Phenomena and Control Flap Effectiveness, 1995, MSc thesis, Cranfield College of Aeronautics.
3. ELFSTROM, G.M. Turbulent separation in hypersonic flow, 1971, I.C. Aero Report 71-16, Dept of Aeronautics, Imperial College of Science & Technology.
4. ELFSTROM, G.M. Turbulent hypersonic flow at a wedge-compression corner, *J Fluid Mech*, 1972, **53**, pp 113-127.
5. COLEMAN, G.T. Hypersonic Turbulent Boundary Layer Studies, March 1973, PhD Thesis, Department of Aeronautics, Imperial College of Science & Technology.
6. STOLLERY, J.L. and COLEMAN, G.T. A correlation between pressure and heat transfer distributions at supersonic and hypersonic speeds, *Aero Q*, November 1975, pp 304-312.
7. COLEMAN, G.T. and STOLLERY, J.L. Heat transfer from hypersonic shock wave/turbulent boundary layer interactions, *J Fluid Mech*, 1972, **56**, pp 741-752.
8. BOGDONOFF, S.M. and KEPLER, C.E. Separation of a supersonic turbulent boundary layer, *J Aero Sciences*, June 1955, pp 414-424.
9. HOLDEN, M.S. Shock-wave/turbulent boundary layer interaction in hypersonic flow, January 1977, AIAA Paper 77-45.
10. SPAID, F.W. and FRISHNETT, J.C. Incipient separation of a supersonic turbulent boundary layer including effects of heat transfer, *AIAA J*, July 1972, **10**, (7), pp 915-922.
11. BATHAM, J.P. An experimental study of turbulent separating & reattaching flows at a high Mach number, *J Fluid Mech*, 1972, **52**, Part 3, pp 425-435.
12. MILLER, D.S., HIJMAN, R. and CHILDS, M.E. Mach 8 to 22 studies of flow separation due to deflected control surfaces, *AIAA J*, February 1964, **2**, (2).
13. KNIGHT, D., YAN, H., PANARAS, A. and ZHELTOVODOV, A. Advances in CFD prediction of shock wave turbulent boundary layer interactions, *Prog in Aerospace Sci*, February/April 2003, **39**, (2-3), pp 121-184.
14. SCHLICHTING, H. *Boundary Layer Theory*, Chapter XI, 1956, McGraw-Hill.
15. BERTIN, J.J., HAYDEN, T.E. and GOODRICH, W.D. Shuttle boundary layer transition due to distributed roughness and surface cooling, *J Spacecraft & Rockets*, September-October 1982, **19**, (5), pp 389-396.
16. DISIMILE, P.J. and SCAGGS, N.E. An investigation into wedge induced turbulent boundary layer separation on a uniformly roughened surface at Mach 6, 1989, AIAA 89-2163-CP, pp 32-41, Proceedings of the Seventh AIAA Applied Aerodynamics Conference, 31 July-2 August, 1989, Seattle, Washington.
17. CHRISTOPH, G.H. and FIORE, A.W. Numerical simulation of flow over rough surfaces including effects of shock waves, February 1975, ARL Tech Report 75-0028.
18. BABINSKY, H. A Study of Roughness in Turbulent Hypersonic Boundary Layers, 1993, PhD thesis, Cranfield University.
19. MCCONNELL, A.D. Roughness effects on impinging shock wave/ turbulent boundary layer interactions, August 1999, MPhil thesis, Cambridge University.
20. BABINSKY, H., INGER, G.R. and MCCONNELL, A.D. A basic experimental/theoretical study of rough wall turbulent shock/boundary layer interaction, 1999, Paper 0050, Proceedings of the 22nd International Symposium on Shock Waves, Imperial College, London, 18-23 July, 1999.